ChemComm

COMMUNICATION

View Article Online
View Journal | View Issue

Cite this: *Chem. Commun.*, 2016, 52, 7221

Received 22nd January 2016,
Accepted 16th March 2016

DOI: 10.1039/c6cc00660d

www.rsc.org/chemcomm

Positron detection in silica monoliths for miniaturised quality control of PET radiotracers†

Mark D. Tarn,‡[ab] Dzmitry Maneuski,‡*[c] Richard Alexander,§[d] Nathaniel J. Brown,[d] Val O'Shea,[c] Sally L. Pimlott,[e] Nicole Pamme*[b] and Stephen J. Archibald*[ab]

We demonstrate the use of the miniaturised Medipix positron sensor for detection of the clinical PET radiotracer, [^{68}Ga]gallium-citrate, on a silica-based monolith, towards microfluidic quality control. The system achieved a far superior signal-to-noise ratio compared to conventional sodium iodide-based radio-HPLC detection and allowed real-time visualisation of positrons in the monolith.

Positron emission tomography (PET) is a powerful medical imaging technique with unrivalled sensitivity, and is used for diagnostic imaging in oncology, cardiology and neurology.[1,2] Radiotracers are molecules labelled with positron-emitting radioisotopes (*e.g.* ^{11}C, ^{18}F or ^{68}Ga) that are used in PET imaging. The current standard production method for the most commonly used radiotracer ([^{18}F]fluorodeoxyglucose) is to generate it in large batches and then transport to imaging centres. However, this form of centralised production limits the number of different radiotracers available and precludes responsive imaging, limiting the scope of clinical investigations. In recent years, the concepts of decentralised production[3] and dose-on-demand[4–6] radiotracer synthesis have gained interest in the move towards stratified patient treatment, wherein a single dose of an appropriate tracer would be generated for a specific patient. The most feasible route to this is *via* microfluidic platforms,[7] but while on-chip synthesis of some radiotracers has been demonstrated,[8,9] miniaturisation of the subsequent quality control (QC) steps onto an integrated lab-on-a-chip microfluidic device has not been achieved.

We are developing an integrated microfluidic platform for the miniaturised QC testing of PET radiopharmaceuticals, with a view to short analysis times, low sample volumes, and minimal radiation exposure to operating staff. Many of the necessary QC tests require the separation and radiodetection of sample components *via* thin layer chromatography (radio-TLC) or high performance liquid chromatography (radio-HPLC).[10,11] Silica-based monoliths have recently become popular for chromatography,[12] including quality control in pharmaceutical production,[13] and have proven successful in a variety of microfluidic applications.[14] As such, they have great potential in the microfluidic QC testing of PET radiotracers. However, the requirement to detect radioactivity in such a miniaturised separation system brings further challenges.

While several examples of on-chip radiodetection can be found in the literature, including phosphor imaging,[15] Cerenkov light detection,[16] imaging with plastic[17] or inorganic scintillators,[18,19] solid-state beta-particle cameras,[20] PIN photodiode arrays,[21] and liquid scintillator-containing microchannels interfaced to a PMT,[22] these methods can suffer from a variety of issues including slow response times, low sensitivity, high cost, and/or complexity of fabrication. Here, we present the first application of a Medipix-based positron sensor[23] for the detection of radioactivity in silica-based monoliths (Fig. 1) towards miniaturisation of QC testing.

The Medipix2 sensor is a hybrid silicon pixel detector capable of direct positron detection that was originally developed within the high energy particle physics community at the European Organization for Nuclear Research (CERN).[24] Featuring a 65k single-photon counting pixel array with a square pixel size of 55 μm, on a 14 × 14 mm^2 detection area, the sensor can act as a real-time camera for positrons. This feature, combined with the sensor's small size, makes it an ideal candidate for on-chip radiodetection. Herein, we evaluate its potential by studying the passage of gallium-68 solutions[25,26] through silica-based monoliths[12,27]

[a] *Positron Emission Tomography Research Centre, University of Hull, Cottingham Road, Hull, HU6 7RX, UK. E-mail: s.j.archibald@hull.ac.uk; Fax: +44 (0)1482 466410; Tel: +44 (0)1482 465488*
[b] *Department of Chemistry, University of Hull, Cottingham Road, Hull, HU6 7RX, UK. E-mail: n.pamme@hull.ac.uk; Fax: +44 (0)1482 466410; Tel: +44 (0) 1482 465027*
[c] *School of Physics and Astronomy, University of Glasgow, Glasgow, G12 8QQ, UK. E-mail: dima.maneuski@glasgow.ac.uk*
[d] *School of Engineering, University of Hull, Cottingham Road, Hull, HU6 7RX, UK*
[e] *School of Medicine, University of Glasgow, Glasgow, G12 8QQ, UK*

† Electronic supplementary information (ESI) available: Experimental details, results of ^{68}Ga-citrate injections, and videos of Medipix recordings. See DOI: 10.1039/c6cc00660d

‡ Authors contributed equally to this work.

§ Current address: Centre for Regional and Rural Futures, Faculty of Science, Engineering and Built Environment, Deakin University, Geelong, Victoria, 3216, Australia.

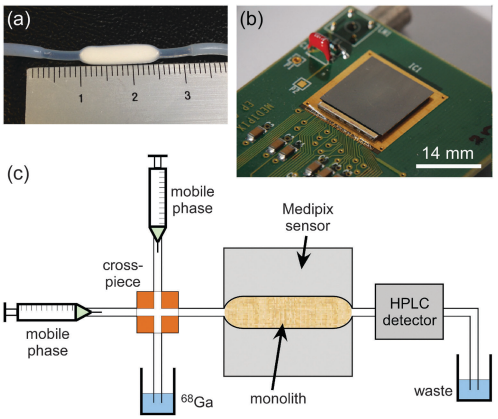

Fig. 1 (a) Silica-based monolithic column encased in heat-shrink tubing. (b) Medipix positron detector, featuring a 14 × 14 mm^2 sensor area. (c) Schematic of the experimental setup, with the monolith placed above the Medipix sensor, and featuring a cross-injection system and a standard sodium iodide radio-HLPC detector.

designed for purification and chromatographic separation in a future integrated microfluidic QC platform.

Since positrons can only travel a short distance before annihilation with an electron (up to several mm dependent on the positron energy),[28] an initial study was performed to determine the effect of distance between a radioisotope and the positron detector. Microscope cover slips (150 μm thickness) were stacked on top of the sensor in order to vary the glass thickness between the detection area and the fluorine-18 ($t_{\frac{1}{2}}$ = 109.7 min) radioisotope solution (see Fig. S1a, ESI†). Fluorine-18 was used initially as it has a low positron energy compared to the other common PET isotopes (^{18}F positron end point energy of 634 keV compared to 961 keV and 1899 keV for the positron emitted from ^{11}C and ^{68}Ga, respectively)[29] and therefore represents a worst case scenario in terms of positron penetration distance. A 20 μL droplet of fluorine-18 was pipetted onto the cover slip stack (Fig. S1a in the ESI†), with thickness varied from 150 μm to 900 μm, and the resultant signal was counted for 600 s, with an acquisition time of 0.1 s. The Medipix was operated in "counting" mode rather than "integration" mode, enabling higher signal-to-noise ratios compared to other detectors that employ the latter mode. A low energy level threshold was set to just above the noise level of the detector (equivalent to 4.5 keV X-ray), with no high threshold level applied. The results (see Fig. S1b–h, ESI†) clearly demonstrated the expected decrease in signal intensity as the distance between the radioisotope and sensor was increased and so more positrons had annihilated prior to reaching the detector surface. Nonetheless, even at the maximum distance tested of 900 μm, positron signals could still be detected.

The next step was to determine the positron detector's sensitivity to gallium-68 ($t_{\frac{1}{2}}$ = 68 min). A solution of ^{68}Ga-citrate, which is used for PET imaging of inflammation, infection, and tumours,[30,31] was prepared in order to determine the detector's sensitivity to the gallium-68 radioisotope. A length of narrow bore Tygon tubing (254 μm ID, 762 μm OD) was fixed over the sensor area, yielding a detection volume of 709 nL and distance between the sensor and the radioisotope of 254 μm. The tubing was filled *via* syringe with

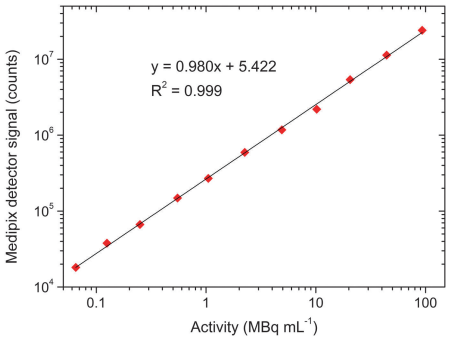

Fig. 2 Plot showing the linearity of the positron detection signal with varying radioactivity levels of the ^{68}Ga-citrate radiotracer on a log scale.

^{68}Ga-citrate solutions of varying activity levels, and 100 frames of the detector response were recorded (1.0 s integration time). The results are shown in Fig. 2, and demonstrate excellent linearity of signal with activity levels (in MBq mL^{-1}). The data is also shown replotted on a linear scale in Fig. S2 (ESI†). For comparison, a clinical PET scan typically requires around 370 MBq (10 mCi), and so assuming a maximum injection volume of about 10 mL the expected activity levels during purification and quality control would be a minimum of 37 MBq mL^{-1}. With this in mind, the positron detector was able to detect clinically relevant levels of activity in volumes of hundreds of nanolitres.

Subsequently, tests were performed to determine whether the detector was capable of detecting injected plugs of activity as they flowed through a monolithic column, with a view towards monolithic radio-TLC and radio-HPLC applications. Porous silica monoliths were prepared as described in the literature[32] and moulded such that they had a thin but flat shape (14 mm long × 4 mm wide × 1.5 mm thick). This shape was designed to restrict the monolith length to the dimensions of the detector area, while limiting the number of undetected positrons by keeping the monolith thin. Following fabrication, monoliths were encased in PTFE heat-shrink tubing (1.27 mm ID, 1.87 mm OD) that allowed it be connected to a flow system, and the monolith was fixed onto the positron detector area. The monolith was connected at one end to a sample injection system comprising two syringe pumps and a four-way cross-piece (Fig. 1c and Fig. S3, ESI†). The other end of the monolith tubing was connected to a conventional 1″ sodium iodide crystal (NaI)/photomultiplier tube (PMT) radio-HPLC detector (PN-FXX-03 NaI/PMT, Dual Scan-RAM, LabLogic Systems Ltd, UK), which detects the 511 keV gamma rays produced by positron annihilation, for direct comparison of detection signals.

Solutions of ^{68}Ga-citrate were prepared and then injected into the monolith by first drawing the solution through the cross-piece perpendicular to the direction of the silica monolith, then halting that flow and applying flow in the direction of the monolith (see Fig. S4, ESI†). This allowed injection of a plug of ^{68}Ga-citrate of ~17 nL, based on the cross-piece dimensions. Four injections were performed in 0.1 M citric acid solution with varying ^{68}Ga-citrate activities (6–15 MBq mL^{-1}, yielding 101–254 Bq in 17 nL) and flow rates (50 and 200 μL min^{-1}), with the sample first passing through the monolith for detection *via* the positron

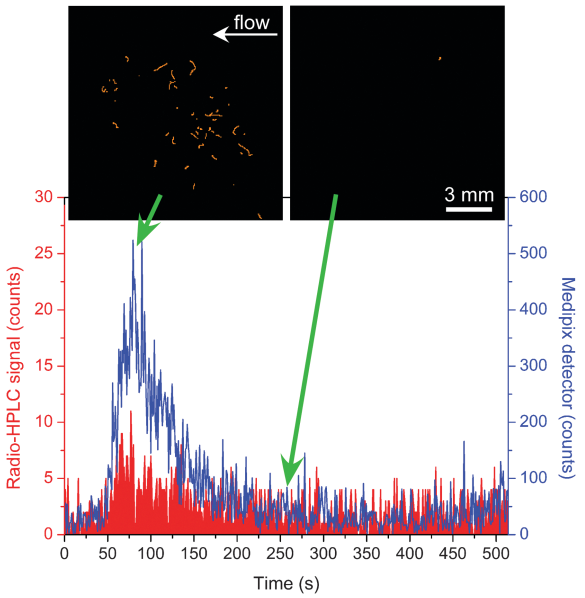

Fig. 3 Plot of ^{68}Ga-citrate radioactive emissions as it passed through the monolithic column. The blue signal shows the signal from the positron detector below the monolith, while the red signal was taken from a flow-through NaI/PMT radio-HPLC detector. Note that the plots are on different scales. Inset are images (14 × 14 mm^2) taken from the detector at different time points.

detector, then passing through the NaI/PMT radio-HPLC detector. The integration time of each detector was set to 1 second. Fig. 3 shows the results from one of the injections (15 MBq mL^{-1}, 200 μL min^{-1}), with the blue signal from the positron detector and the red signal from the NaI/PMT radio-HPLC detector (note that they are on different scales). The positron detector clearly shows a significant increase in detection signal for the ^{68}Ga-citrate peak compared to the radio-HPLC detector, but also demonstrates a substantial increase in the signal-to-noise (S/N) ratio of 14 for the positron detector and 3 for the radio-HPLC detector. Thus, not only was the positron sensor capable of detecting activity in real-time as it passed through a monolith, but also that its performance was vastly superior to standard detectors. Fig. 3 (and the video labelled "1-Ga68 injection 1" in the ESI†) also shows images taken from the positron detector as the ^{68}Ga-citrate plug first passed through the monolith and after the plug had finished passing through. The tracks of the positrons can clearly be seen on the first image, demonstrating the characteristic "random-walk" motion of the positrons.

The positron detector and radio-HPLC signals for all four injections of ^{68}Ga-citrate are shown in Fig. S5 and S6 (ESI†) (plotted on different scales to show differences in signal intensity and S/N ratio, respectively), and the videos of the positron detection signals for each injection have been included in the ESI.† The resultant S/N ratios are shown in Table S2 (ESI†). While the radio-HPLC signals had S/N ratios ranging from 3 to 7, those of the positron detector ranged from a minimum of 10 to a far superior 48. The wide range of S/N ratios for the positron detector is due to improvements to the manual sample injections as a result of practice over the course of the tests, and makes clear the need for optimisation of the injection system. All of these aspects could be investigated in future tests. It is evident, however, that while the conventional NaI/PMT radio-HPLC detector was nearing its limits at the levels of activity being analysed, the positron detector was more than capable of detecting these low levels in real-time in very small volumes of solution. These results highlight the great potential for this detection system for use in microfluidic systems, whilst also having the advantage of visualising the activity rather than only detecting a signal. The positron detection images shown in Fig. 3 and 4 also demonstrate very limited sensitivity to gamma rays emitted upon annihilation of the positrons with electrons. Hence, unlike a conventional NaI/PMT gamma detector, no shielding is required for the positron detector, ensuring a simple setup with a small footprint.

In a final test, the ability to monitor the trapping and release of gallium-68 on the silica monolith was investigated. A solution of ^{68}Ga^{3+} was prepared as ^{68}GaCl$_3$ and loaded into the cross-piece of the sample injection setup as described earlier. The solution was then injected into the monolith at 50 μL min^{-1} in a mobile phase of sodium phosphate (0.4 M). Fig. 4a shows the build-up of ^{68}Ga^{3+} (11 MBq mL^{-1}) over time as it became trapped at the start of the monolith. However, when the mobile phase was then changed to 0.1 M citric acid (at 50 μL min^{-1}), the gallium-68 was eluted from the monolith and successfully monitored using the positron

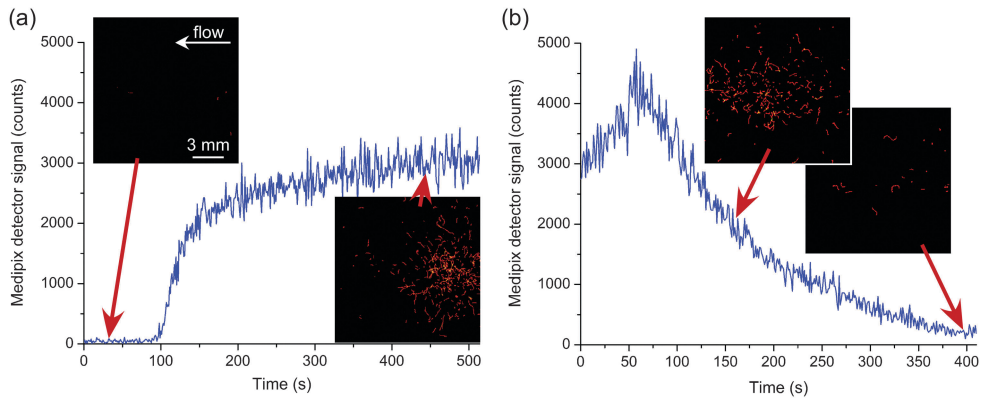

Fig. 4 Trap and release of ^{68}Ga^{3+} on the silica-based monolith, with the positron detector showing the activity in real-time. (a) Trapping in phosphate solution (0.4 M). (b) Release in citric acid (0.1 M). The flow of solution was right-to-left in the images.

detector (Fig. 4b). Videos of these processes ("5-Trapping of 68Ga" and "6-Release of 68Ga") obtained *via* the positron detector can be found in the ESI.†

In summary, we have demonstrated, for the first time, the monitoring of gallium-68 solutions in silica monoliths in a flow-based system using a small-footprint Medipix positron detector with real-time visualisation. The detector yielded far superior signal-to-noise ratios compared to a conventional radio-HPLC detector for the measurement of the ^{68}Ga-citrate PET radiotracer. Crucially, no shielding is required since it detects only short-ranged positrons rather than gamma rays. Variants of the Medipix detector can be purchased commercially (*e.g.* from Advacam, X-Ray Imatek or Jablotron) for not a great deal more than conventional detectors, although licensing and terms of use must be considered. These factors make the platform ideal for miniaturised, monolith-based radio-TLC and radio-HPLC applications in an integrated microfluidic QC system.

M. D. T., R. A., N. J. B., N. P. and S. J. A. acknowledge the Daisy Appeal charity (grant no. DAhul2011) and HEIF (University of Hull) for funding, and thank Dr Assem Allam and his family for the generous donation to help found the PET Research Centre at the University of Hull and for their continued support. The authors thank Benjamin P. Burke and Gonçalo S. Clemente for preparation of the gallium-68 radioisotope solutions, and Ping He for assistance with monolith production. This work has been partially supported by the STFC (grant ST/K001205/1).

Notes and references

1 S. L. Pimlott and A. Sutherland, *Chem. Soc. Rev.*, 2011, **40**, 149–162.
2 M. E. Phelps, *Annu. Rev. Nucl. Part. Sci.*, 2002, **52**, 303–338.
3 P. Y. Keng, M. Esterby and R. M. Van Dam, Micro-reactors for PET tracer labeling, in *Positron Emission Tomography – Current Clinical and Research Aspects*, ed. C.-H. Hsieh, InTech, 2012.
4 G. Pascali, G. Mazzone, G. Saccomanni, C. Manera and P. A. Salvadori, *Nucl. Med. Biol.*, 2010, **37**, 547–555.
5 V. Arima, G. Pascali, O. Lade, H. R. Kretschmer, I. Bernsdorf, V. Hammond, P. Watts, F. De Leonardis, M. D. Tarn, N. Pamme, B. Z. Cvetkovic, P. S. Dittrich, N. Vasovic, R. Duane, A. Jaksic, A. Zacheo, A. Zizzari, L. Marra, E. Perrone, P. A. Salvadori and R. Rinaldi, *Lab Chip*, 2013, **13**, 2328–2336.
6 V. Awasthi, J. Watson, H. Gali, G. Matlock, A. McFarland, J. Bailey and A. Anzellotti, *Appl. Radiat. Isot.*, 2014, **89**, 167–175.
7 M. D. Tarn and N. Pamme, Microfluidics, in *Elsevier Reference Module in Chemistry, Molecular Sciences and Chemical Engineering*, ed. J. Reedijk, Elsevier, Waltham, MA, 2013.
8 G. Pascali, P. Watts and P. A. Salvadori, *Nucl. Med. Biol.*, 2013, **40**, 776–787.
9 C. Rensch, A. Jackson, S. Lindner, R. Salvamoser, V. Samper, S. Riese, P. Bartenstein, C. Wängler and B. Wängler, *Molecules*, 2013, **18**, 7930–7956.
10 J. C. Hung, *J. Nucl. Med.*, 2002, **43**, 1495–1506.
11 S. Yu, *Biomed. Imaging Intervention J.*, 2006, **2**, e57.
12 Z. Walsh, B. Paull and M. Macka, *Anal. Chim. Acta*, 2012, **750**, 28–47.
13 C. K. Zacharis, *J. Chromatogr. Sci.*, 2009, **47**, 443–451.
14 M. Vázquez and B. Paull, *Anal. Chim. Acta*, 2010, **668**, 100–113.
15 M. Lavén, S. Wallenborg, I. Velikyan, S. Bergström, M. Djodjic, J. Ljung, O. Berglund, N. Edenwall, K. E. Markides and B. Långström, *Anal. Chem.*, 2004, **76**, 7102–7108.
16 J. S. Cho, R. Taschereau, S. Olma, K. Liu, Y.-C. Chen, C. K. F. Shen, R. M. van Dam and A. F. Chatziioannou, *Phys. Med. Biol.*, 2009, **54**, 6757–6771.
17 J. S. Cho, N. T. Vu, Y. H. Chung, Z. T. Yu, R. W. Silverman, R. Taschereau, H. R. Tseng and A. F. Chatziioannou, *IEEE 2006 Nuclear Science Symposium Conference Record*, San Diego, CA, 2006.
18 J. S. Cho, N. T. Vu, Z. T. F. Yu, R. W. Silverman, R. Taschereau, T. Hsian-Rong and A. F. Chatziioannou, *IEEE 2007 Nuclear Science Symposium Conference Record*, Honolulu, HI, 2007.
19 S. Türkcan, J. Nguyen, M. Vilalta, B. Shen, F. T. Chin, G. Pratx and P. Abbyad, *Anal. Chem.*, 2015, **87**, 6667–6673.
20 N. T. Vu, Z. T. F. Yu, B. Comin-Anduix, J. N. Søndergaard, R. W. Silverman, C. Y. N. Chang, A. Ribas, H.-R. Tseng and A. F. Chatziioannou, *J. Nucl. Med.*, 2011, **52**, 815–821.
21 L. Convert, F. G. Baril, V. Boisselle, J.-F. Pratte, R. Fontaine, R. Lecomte, P. G. Charette and V. Aimez, *Lab Chip*, 2012, **12**, 4683–4692.
22 A. Mapelli, B. Gorini, M. Haguenauer, S. Jiguet, G. L. Miotto, W. Vandelli, N. V. Triviño and P. Renaud, *Sens. Actuators, A*, 2010, **162**, 272–275.
23 D. Maneuski, F. Giacomelli, C. Lemaire, A. Luxen, V. O'Shea, J. Owens, S. Pimlott and A. Plenevaux, *Phys. Med. Biol.*, 2016, in press.
24 X. Llopart, M. Campbell, R. Dinapoli, D. San Segundo and E. Pernigotti, *IEEE Trans. Nucl. Sci.*, 2002, **49**, 2279–2283.
25 B. P. Burke, G. S. Clemente and S. J. Archibald, *J. Labelled Compd. Radiopharm.*, 2014, **57**, 239–243.
26 T. J. Wadas, E. H. Wong, G. R. Weisman and C. J. Anderson, *Chem. Rev.*, 2010, **110**, 2858–2902.
27 H. Kobayashi, T. Ikegami, H. Kimura, T. Hara, D. Tokuda and N. Tanaka, *Anal. Sci.*, 2006, **22**, 491–501.
28 P. Peller, R. Subramaniam and A. Guermazi, *PET-CT and PET-MRI in Oncology: A Practical Guide*, Springer, Heidelberg, 2012.
29 Decay Data Evaluation Project (DDEP), Laboratoire National Henri Becquerel, www.nucleide.org/DDEP_WG/DDEPdata.htm, accessed August 2015.
30 A. Rizzello, D. Di Pierro, F. Lodi, S. Trespidi, G. Cicoria, D. Pancaldi, C. Nanni, M. Marengo, M. C. Marzola, A. Al-Nahhas, D. Rubello and S. Boschi, *Nucl. Med. Commun.*, 2009, **30**, 542–545.
31 B. P. Burke, N. Baghdadi, A. E. Kownacka, S. Nigam, G. S. Clemente, M. M. Al-Yassiry, J. Domarkas, M. Lorch, M. Pickles, P. Gibbs, R. Tripier, C. Cawthorne and S. J. Archibald, *Nanoscale*, 2015, **7**, 14889–14896.
32 P. I. Fletcher, S. Haswell, P. He, S. Kelly and A. Mansfield, *J. Porous Mater.*, 2011, **18**, 501–508.

